MPI-PhE/2001-11
June 15, 2001

Measurement of the longitudinal and transverse cross-section in e^+e^- annihilation at $\sqrt{s} = 35$-44 GeV

M. Blumenstengel[(1)], O. Biebel[(1)], P.A. Movilla Fernández[(1)], P. Pfeifenschneider[(1,a)], S. Bethke[(1)], S. Kluth[(1)] and the JADE Collaboration[(2)]

Abstract

An investigation of the polar angle distribution of charged hadrons is presented using data taken by the JADE experiment at the PETRA e^+e^- collider at centre-of-mass energies of 35 and 44 GeV. From fits to the polar angle distribution the longitudinal, σ_L, and transverse, σ_T, cross-section relative to the total hadronic are determined at an average energy scale of 36.6 GeV. The results are

$$\frac{\sigma_L}{\sigma_{\rm tot}} = 0.067 \pm 0.013 \quad , \qquad \frac{\sigma_T}{\sigma_{\rm tot}} = 0.933 \mp 0.013$$

where total errors are given and the results are exactly anti-correlated. Using the next-to-leading order QCD prediction for the longitudinal cross-section, the value

$$\alpha_S(36.6 \text{ GeV}) = 0.150 \pm 0.025$$

of the strong coupling constant is obtained in agreement with the world average value of α_S evolved to an energy scale of 36.6 GeV.

Submitted to Phys. Lett. B

(1) Max-Planck-Institut für Physik, D-80805 München, Germany
contact e-mail: biebel@mppmu.mpg.de
(2) for a full list of members of the JADE Collaboration see Reference [1]
(a) now at SAP Deutschland AG & Co. KG, Neurottstraße 15, 69190 Walldorf, Germany

1 Introduction

The energy and the momentum spectrum of a hadron h produced in the annihilation process $\mathrm{e}^+\mathrm{e}^- \rightarrow \gamma, \mathrm{Z} \rightarrow h + X$ is described by a fragmentation function $\mathcal{F}^h(x) \equiv (1/\sigma_{\mathrm{tot}}) \cdot (\mathrm{d}\sigma^h/\mathrm{d}x)$. Here x is either the fractional momentum, $x_p \equiv 2p/\sqrt{s}$, or the fractional energy, $x_E \equiv 2E/\sqrt{s}$, carried by a hadron h, and $\sqrt{s}$ is the centre-of-mass energy of the annihilation process with total hadronic cross-section σ_{tot}. In the case of unpolarized $\mathrm{e}^\pm$ beams, and averaging over the polarization of the hadron h, the fragmentation function receives contributions from the transverse (T) and longitudinal (L) polarization states of the intermediate electroweak vector bosons, γ and Z, and from their interference yielding an asymmetric contribution (A). The most general form of the differential cross-section for the inclusive single-particle production in $\mathrm{e}^+\mathrm{e}^-$ annihilation is [2, 3]

$$\frac{1}{\sigma_{\mathrm{tot}}} \cdot \frac{\mathrm{d}^2\sigma^h}{\mathrm{d}x\ \mathrm{d}(\cos\theta)} = \frac{3}{8}\left(1+\cos^2\theta\right) \cdot \mathcal{F}_T^h(x) + \frac{3}{4}\left(\sin^2\theta\right) \cdot \mathcal{F}_L^h(x) + \frac{3}{4}\left(\cos\theta\right) \cdot \mathcal{F}_A^h(x) \quad , \tag{1}$$

where θ is the polar angle between the direction of the incoming e^- and the outgoing hadron h. At centre-of-mass energies much larger than the mass of the produced quark q, the longitudinal contribution is negligible [4] due to the helicity structure at the quarks' production vertex. A sizeable contribution to the longitudinal fragmentation function, however, comes from gluon radiation from the $q\bar{q}$ system in the final state [2]. The asymmetric contribution is largest at energies below and above but very small at the Z peak. Even though it is 20-30% of the transverse cross-section [4] in the energy range of 35 through 44 GeV considered for this analysis, the required experimental distinction of quark and antiquark renders a measurement of the asymmetric contribution virtually impossible. It, therefore, was not considered for this analysis.

The fragmentation functions are related to the perturbatively calculable ratios of the longitudinal, σ_L, and transverse, σ_T, cross-sections to the total cross-section. Integrating Eq. (1) over $\cos\theta$ and respecting energy conservation for the integral over x yields [2]

$$\frac{1}{2}\sum_h \int \mathrm{d}x\ x \cdot \frac{1}{\sigma_{\mathrm{tot}}} \cdot \frac{\mathrm{d}\sigma^h}{\mathrm{d}x} = \frac{\sigma_T}{\sigma_{\mathrm{tot}}} + \frac{\sigma_L}{\sigma_{\mathrm{tot}}} = 1 \quad , \tag{2}$$

where

$$\frac{\sigma_{T,L}}{\sigma_{\mathrm{tot}}} \equiv \frac{1}{2}\sum_h \int \mathrm{d}x\ x \cdot \mathcal{F}_{T,L}^h(x) \quad . \tag{3}$$

The contribution of gluon radiation to $\sigma_{T,L}/\sigma_{\mathrm{tot}}$ has been calculated in second order of α_S [5]. At first order the QCD correction in the total cross-section contributes only to the longitudinal part [2]:

$$\sigma_{\mathrm{tot}} = \sigma_T + \sigma_L = \left(\sigma_0 + \mathcal{O}(\alpha_S^2)\right) + \left(\frac{\alpha_S}{\pi}\sigma_0 + \mathcal{O}(\alpha_S^2)\right) \quad , \tag{4}$$

where σ_0 is the Born level cross-section. This allows tests of QCD and determinations of α_S from measurements of $\sigma_L/\sigma_{\mathrm{tot}}$ and $\sigma_T/\sigma_{\mathrm{tot}}$.

The longitudinal and transverse fragmentation functions were already investigated by the SLAC/LBL magnetic detector collaboration at the SPEAR collider at 7.4 GeV [6], by the TASSO collaboration at the PETRA collider at 14, 22, and 34 GeV [7], and by the OPAL, ALEPH, and DELPHI collaborations at the LEP collider at $\sqrt{s} \approx m_{\mathrm{Z}}$ [8–10]. Ratios $\sigma_L/\sigma_{\mathrm{tot}}$ to derive $\alpha_S(m_{\mathrm{Z}})$ were only determined by the OPAL and DELPHI collaborations [8, 10].

Due to the sum rule Eq. (2) all details of the unknown fragmentation functions disappear from the longitudinal and transverse cross-sections up to corrections suppressed by some power of $1/\sqrt{s}$. A measurement of these cross-sections at centre-of-mass energies different from $\sqrt{s} \approx m_{\mathrm{Z}}$

description	cut
minimum track momentum	$p > 0.1$ GeV
tracks coming out of a cylinder ($\varnothing$ 3 cm $\times$7 cm) around the e^+e^- vertex	$n_{\rm ch}^{\rm vertex} \geq 4$
tracks having $\geq$ 24 points and $p_t > 500$ MeV	$n_{\rm ch} \geq 3$
visible energy	$E_{\rm vis} = \sum_i E_i > \sqrt{s}/2$
longitudinal momentum balance	$p_{\rm bal} = \lvert \sum p_i^z / E_{\rm vis} \rvert < 0.4$
axial vertex position	$\lvert z_{\rm VTX} \rvert < 150$ mm
polar angle of thrust axis	$\lvert \cos\theta_T \rvert < 0.8$
total missing momentum	$p_{\rm miss} = \lvert \sum \vec{p}_i \rvert < 0.3 \cdot \sqrt{s}$

Table 1: The main cuts are listed for the selection of multihadronic events which were varied to assess systematic uncertainties (see text). E_i and $\vec{p}_i$ are energy and 3-momentum of tracks and clusters.

year	$\sqrt{s}$ [GeV]	data	MC
1979-1985	34-36	13 013	19 814
1986	34-36	20 926	25 123
1984/85	43-45	4504	14 497

Table 2: Number of selected multihadronic events in data and Monte Carlo detector simulation (MC).

is, therefore, indispensable to experimentally investigate the question whether power corrections to Eq. (4) are required and whether these are of the form $1/\sqrt{s}$ or $1/s$ [11].

The analysis presented in the following determines $\sigma_L/\sigma_{\rm tot}$, $\sigma_T/\sigma_{\rm tot}$, and α_S at an average energy of $\langle\sqrt{s}\rangle = 36.6$ GeV. It uses data measured with the JADE detector [1, 12] at the PETRA collider to be introduced in Section 2. The measurement of the $\cos\theta$ distribution and the investigation of the experimental systematics are detailed in Section 3. Section 4 presents the results from the fits to the measured $\cos\theta$ distribution. Power corrections to Eq. (4) are considered in Section 5. Our final results for $\sigma_L/\sigma_{\rm tot}$, $\sigma_T/\sigma_{\rm tot}$, and α_S are summarized in Section 6.

2 Detector and data samples

The investigation presented in this paper is a re-analysis of data recorded by the JADE detector at the PETRA electron-positron collider. The JADE detector is described in detail elsewhere [1, 12]. The main component of the detector used for this study is the central jet chamber which measured the tracks of charged particles with 8 up to 48 points in about 97% of the full solid angle. The relative resolution of the transverse track momentum was

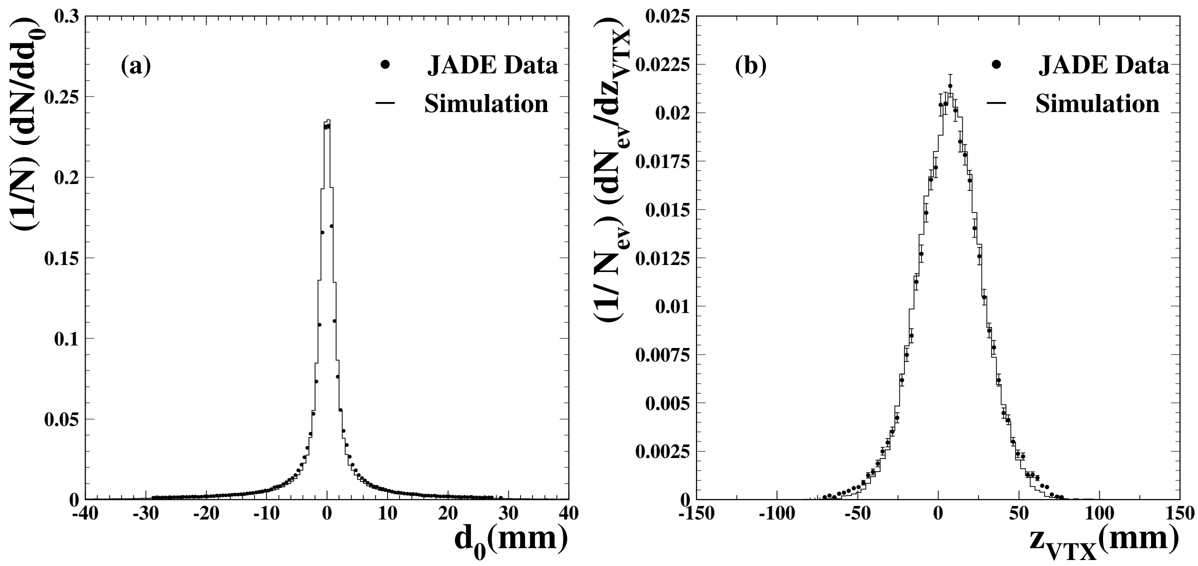

Figure 1: The distributions of (a) the tracks' radial distance of closest approach to the vertex, d_0, and (b) the vertex' axial position are shown for data (points) and simulation (histogram) after shifting and smearing (see text).

$\sigma(p_t)/p_t = \sqrt{0.04^2 + (0.018 \cdot p_t[\mathrm{GeV}/c])^2}$. The spatial resolution in the r-φ plane[1] was 180 μm before 1986 and 110 μm for the data measured in 1986 due to the installation of a digital readout system. The resolution along the z axis was 1.6 cm which degraded when the digital readout came into operation.

The data used for this study were recorded between 1979 and 1986 at centre-of-mass energies of $\sqrt{s}$ = 34-36 GeV and $\sqrt{s}$ = 43-45 GeV. Multihadronic events were selected according to the criteria described in [13]. Applying the selection cuts listed in Tab. 1 yielded the number of events in data and Monte Carlo simulation (MC) listed in Tab. 2. As in our previous publication [13] we used the JADE collaboration's original Monte Carlo samples of multihadronic events from the JETSET program version 6.3 [14] including a detailed simulation of the JADE detector which were available for these energies.

Since the data at $\sqrt{s}$ = 34-36 GeV were recorded with two different configurations of the JADE detector (see [1]), the distributions of the polar angle obtained from these data sets were corrected separately for detector effects. After noticing a good agreement of the corrected distributions they were combined for the fits.

The simulated data had to be adapted to the experimental position of the e^+e^- collision point (I.P.) and the resolutions of the measured z vertex position, z_{VTX}, and of the minimum radial distance of a track to the I.P., d_0. Fig. 1 shows the comparison of the smeared d_0 and z_{VTX} distributions in the simulation and in the data. In radial direction only a gaussian smearing of 0.8 mm was required while for the z vertex position a smearing of 17.5 mm and a shift of 7.4 mm were needed.

[1]JADE used a cylinder coordinate system with the z axis along the e^- beam direction, the radius r is the distance from the z axis, the azimuthal angle φ is measured from the horizontal plane, and the polar angle θ is measured with respect to the z axis.

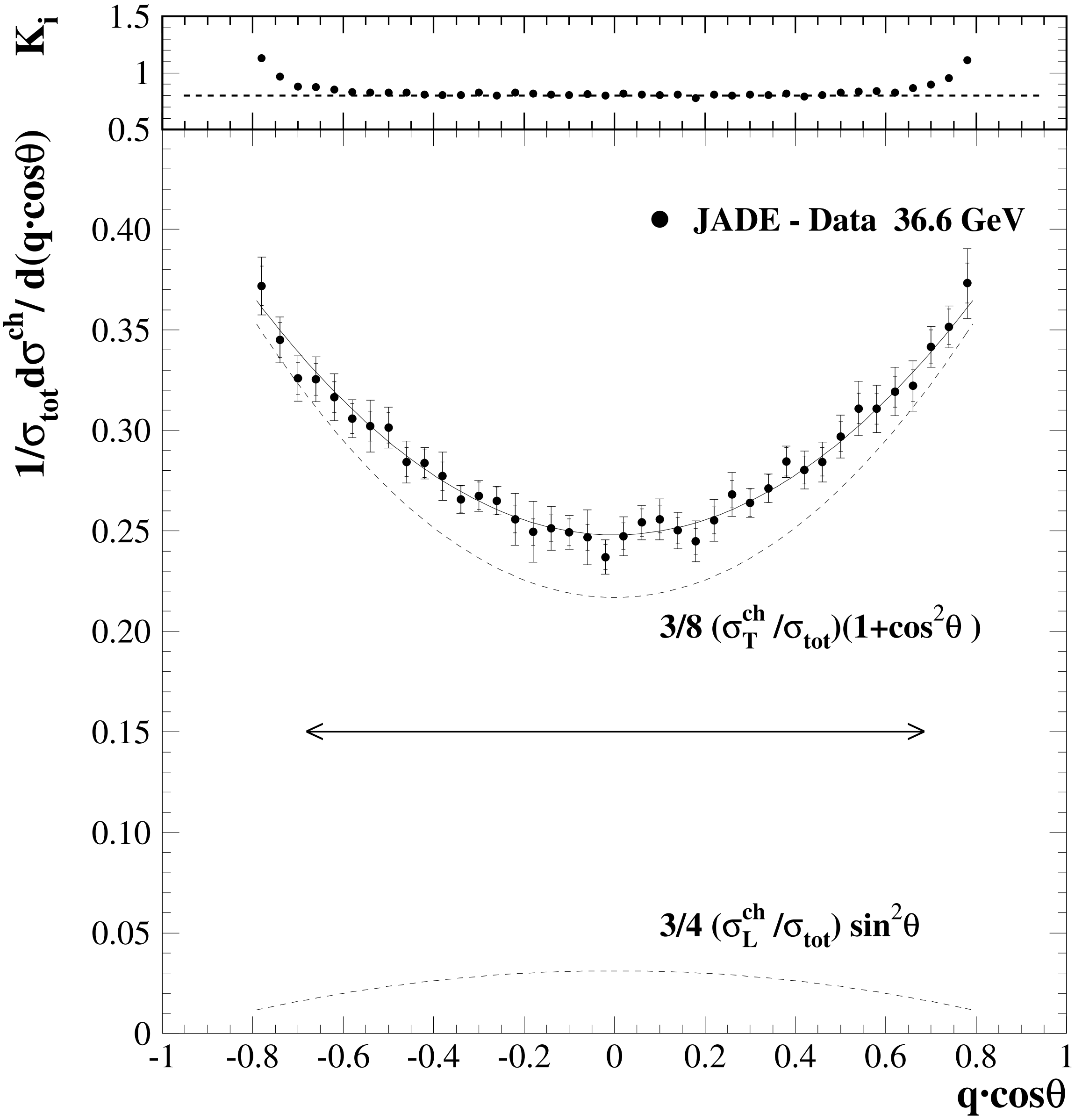

Figure 2: The distribution of $q \cdot \cos\theta$ is shown after correction for detector effects using the factors K_i presented in the upper part of the figure. The inner error bars are the statistical uncertainties due to data and limited detector simulation statistics, and the outer bars are the total errors. The range considered for the fit is indicated by the arrow.

3 Measurement of $\cos\theta$ distribution

To determine the longitudinal and transverse cross-sections the distribution of $\cos\theta$ of all tracks of charged particles was measured. The small correlation of the quark's and the particle's charge indispensible for a determination of the asymmetric cross-section is maintained by multiplying $\cos\theta$ of each particle by the sign q of the particle's charge. Since the experimental sensitivity on the asymmetric contribution is marginal, the fits considered only the longitudinal and transverse contribution to the cross-section which are insensitive to the sign of $q \cdot \cos\theta$.

The effects of limited acceptance and resolution of the detector were corrected using a bin-by-

$q\cdot\cos\theta$ range	$\frac{1}{\sigma_{\rm tot}}\frac{{\rm d}\sigma^{\rm ch}}{{\rm d}(q\cdot\cos\theta)}$
-0.80 - -0.76	$0.372 \pm 0.010 \pm 0.011$
-0.76 - -0.72	$0.345 \pm 0.009 \pm 0.007$
-0.72 - -0.68	$0.326 \pm 0.008 \pm 0.008$
-0.68 - -0.64	$0.326 \pm 0.008 \pm 0.008$
-0.64 - -0.60	$0.316 \pm 0.008 \pm 0.009$
-0.60 - -0.56	$0.306 \pm 0.007 \pm 0.006$
-0.56 - -0.52	$0.302 \pm 0.007 \pm 0.011$
-0.52 - -0.48	$0.301 \pm 0.007 \pm 0.007$
-0.48 - -0.44	$0.284 \pm 0.007 \pm 0.008$
-0.44 - -0.40	$0.284 \pm 0.007 \pm 0.003$
-0.40 - -0.36	$0.277 \pm 0.007 \pm 0.010$
-0.36 - -0.32	$0.266 \pm 0.007 \pm 0.002$
-0.32 - -0.28	$0.267 \pm 0.007 \pm 0.004$
-0.28 - -0.24	$0.265 \pm 0.007 \pm 0.002$
-0.24 - -0.20	$0.256 \pm 0.007 \pm 0.011$
-0.20 - -0.16	$0.250 \pm 0.007 \pm 0.014$
-0.16 - -0.12	$0.251 \pm 0.007 \pm 0.009$
-0.12 - -0.08	$0.249 \pm 0.007 \pm 0.005$
-0.08 - -0.04	$0.247 \pm 0.007 \pm 0.012$
-0.04 - 0.00	$0.237 \pm 0.006 \pm 0.006$

$q\cdot\cos\theta$ range	$\frac{1}{\sigma_{\rm tot}}\frac{{\rm d}\sigma^{\rm ch}}{{\rm d}(q\cdot\cos\theta)}$
0.00 - 0.04	$0.247 \pm 0.007 \pm 0.007$
0.04 - 0.08	$0.254 \pm 0.007 \pm 0.005$
0.08 - 0.12	$0.256 \pm 0.007 \pm 0.008$
0.12 - 0.16	$0.250 \pm 0.007 \pm 0.006$
0.16 - 0.20	$0.245 \pm 0.006 \pm 0.008$
0.20 - 0.24	$0.255 \pm 0.007 \pm 0.008$
0.24 - 0.28	$0.268 \pm 0.007 \pm 0.009$
0.28 - 0.32	$0.264 \pm 0.007 \pm 0.003$
0.32 - 0.36	$0.271 \pm 0.007 \pm 0.002$
0.36 - 0.40	$0.284 \pm 0.007 \pm 0.003$
0.40 - 0.44	$0.280 \pm 0.007 \pm 0.006$
0.44 - 0.48	$0.284 \pm 0.007 \pm 0.007$
0.48 - 0.52	$0.297 \pm 0.007 \pm 0.008$
0.52 - 0.56	$0.311 \pm 0.008 \pm 0.011$
0.56 - 0.60	$0.311 \pm 0.008 \pm 0.009$
0.60 - 0.64	$0.319 \pm 0.008 \pm 0.009$
0.64 - 0.68	$0.322 \pm 0.008 \pm 0.010$
0.68 - 0.72	$0.342 \pm 0.009 \pm 0.006$
0.72 - 0.76	$0.352 \pm 0.009 \pm 0.006$
0.76 - 0.80	$0.373 \pm 0.010 \pm 0.014$

Table 3: The differential $q\cdot\cos\theta$ distribution data are listed for charged particles with statistical and systematic uncertainties. The statistical uncertainties include the uncertainties due to the limited statistics of the detector simulation.

bin correction method. The correction was obtained from the detailed detector simulation as the binwise ratio of the $q\cdot\cos\theta$ distribution at the hadron level and the corresponding distribution at the detector level. Here, hadron level means all charged particles having lifetimes greater than 300 ps generated by the Monte Carlo event generator, and the detector level comprises all charged particles that were observed after passing the simulated events through the detector simulation and reconstruction programs. Effects due to the neutral particles were not corrected using the simulation but were obtained from the measured data as will be detailed in Section 4. Fig. 2 shows the measured distribution of $q\cdot\cos\theta$ after application of the binwise correction factors which are shown in the upper part of the figure. In the central part of the detector the distribution of the correction factors is flat at about 0.8 and increases towards the acceptance boundaries at large $|\cos\theta|$. The values are below unity due to normalizing all distributions to the mean charged multiplicity, in particular those at detector level where the acceptance is reduced by the cut on the polar angle of the thrust axis.

All data sets measured at centre-of-mass energies of about 35 and 44 GeV and corrected for detector effects were combined, weighted with the respective integrated luminosities. The measured values and the statistical and systematic uncertainties are listed in Tab. 3. The corrected distribution is limited to the range of $|\cos\theta| < 0.8$ due to the acceptance limit implied by the cut on the polar angle of the thrust axis.

As an additional cross-check we determined the mean charged multiplicity from the corrected distribution at 35 GeV, yielding $\langle n_{\mathrm{ch}}\rangle = 14.23 \pm 0.04$ where the error is statistical only. This is in agreement within the total error of the published result $\langle n_{\mathrm{ch}}\rangle = 13.6 \pm 0.3(\mathrm{stat.}) \pm 0.6(\mathrm{syst.})$ [15] at this energy where tracks were counted by visually inspecting the events.

To assess the systematic uncertainties due to imperfections of the detector simulation, and due to the contributions from background processes, the main selection cuts listed in Tab. 1 were varied. The measurement of the $q \cdot \cos\theta$ distribution was repeated for each variation and any deviation from the distribution obtained using the standard selection cuts was considered a systematic uncertainty. Tab. 4 summarises all investigated variations of the selection cuts.

Deficiencies of the description of the data by the simulation were considered as a source of systematic uncertainty. The largest deviation to be considered for this investigation is due to the choice of the fragmentation function which yielded more high energetic particles than observed in the data. Its contribution to the systematic error of the $q \cdot \cos\theta$ distribution was obtained from reweighting the simulation to match the fragmentation function of the data prior to determining the correction factors.

Finally, additional selection cuts on d_0 were applied to reject tracks which stem from decays of long-lived particles or from interactions with the detector material. A similar cut on the axial distance of a track to the reconstructed vertex position, z_0, could not be applied since the relevant information is not available in the preprocessed data files [13] we used. Instead we varied the selection cut on the event-by-event vertex position, z_{VTX}, about its average derived from all events, $\langle z_{\mathrm{VTX}}\rangle$. The systematic uncertainty was found from applying tighter cuts on d_0 and z_{VTX} and repeating the measurement. The cuts, $d_0 < 3$ mm or 19 mm, and $|z_{\mathrm{VTX}} - \langle z_{\mathrm{VTX}}\rangle| < 29$ mm or 39 mm, were derived from one and a half and twice the gaussian width of the corresponding distribution measured in the data. The looser cut on d_0, however, was found from fitting an exponential function to the d_0 distribution at large values of d_0. The fit was extended to the largest range describable with this exponential function. The lower end of this fit range was chosen for the looser cut on d_0. This considers that large positive values of d_0 are dominantly due to tracks from decays of long-lived particles such as K^0_S and Λ.

4 Determination of $\sigma_{\mathbf{L}}/\sigma_{\mathbf{tot}}$, $\sigma_{\mathbf{T}}/\sigma_{\mathbf{tot}}$, and $\alpha_{\mathbf{S}}$

From the $q \cdot \cos\theta$ distribution $\sigma_L/\sigma_{\mathrm{tot}}$ and $\sigma_T/\sigma_{\mathrm{tot}}$ can be determined after neutral particles not included in the $q \cdot \cos\theta$ distribution are taken into account. Studies using the JETSET Monte Carlo generator [14] at $\sqrt{s} = 35$ GeV with the parameters quoted in [13,16] yielded

$$\begin{aligned}\left(\eta_L^{\mathrm{ch}}\right)^{\mathrm{had,MC}} &\equiv \left(\frac{\sigma_L^{\mathrm{ch}}}{\sigma_L}\right)^{\mathrm{had,MC}} &=& \quad 0.608 \pm 0.004, \\ \left(\eta_T^{\mathrm{ch}}\right)^{\mathrm{had,MC}} &\equiv \left(\frac{\sigma_T^{\mathrm{ch}}}{\sigma_T}\right)^{\mathrm{had,MC}} &=& \quad 0.6179 \pm 0.0004 \end{aligned} \tag{5}$$

for the ratio of cross-sections obtained from charged and from charged plus neutral particles. Nearly identical ratios were found in [8] using JETSET at $\sqrt{s} = 91.2$ GeV with a different parameter set [17]. Thus, independently of the centre-of-mass energy, the correction of the longitudinal cross-section for neutral particles is expected to be about 1.6% larger than the same correction for the transverse cross-section. Since the correction depends on the details of the hadronization model, and since the absolute difference of the corrections in Eq. (5) is less than the statistical uncertainty of our measurement, the difference was neglected for the determination of the longitudinal and transverse cross-section but was considered for the systematic uncertainties.

Assuming that at the hadron level the correction for neutral particles is identical for the longitudinal and transverse cross-sections, using Eq. (3) the differential cross-section for charged particles given by Eq. (1) can be written as

$$\frac{1}{\sigma_{\mathrm{tot}}} \cdot \frac{\mathrm{d}\sigma^{\mathrm{ch}}}{\mathrm{d}(q \cdot \cos\theta)} = \frac{3}{8}\eta^{\mathrm{ch}} \left[\frac{\sigma_L}{\sigma_{\mathrm{tot}}}\left(1 - 3\cos^2\theta\right) + \left(1 + \cos^2\theta\right)\right] \quad . \tag{6}$$

The unknown parameters to be determined from a fit to the data are η^{ch}, which is the correction factor for the total cross-section accounting for the neutral particles, and $\sigma_L/\sigma_{\mathrm{tot}}$. From the relation known in $\mathcal{O}(\alpha_S^2)$ [5]

$$\left(\frac{\sigma_L}{\sigma_{\mathrm{tot}}}\right)_{\mathrm{PT}} = \frac{\alpha_S}{\pi} + 8.444\left(\frac{\alpha_S}{\pi}\right)^2 \tag{7}$$

a formula similar to Eq. (6) can be derived which allows for a direct determination of the strong coupling constant α_S.

The largest sensitivity to the longitudinal cross-section comes from the central region, $|\cos\theta| \approx 0$, and the forward regions, $|\cos\theta| \to 1$. Since measurements in the forward region are affected by the limited detector acceptance, the central part of the detector, $|\cos\theta| < 0.68$, was chosen for the range of the fit. For this fit range a good fit was obtained with $\chi^2/\mathrm{d.o.f.} \approx 0.49$.[2] The two fits yielded

$$\frac{\sigma_L}{\sigma_{\mathrm{tot}}} = 0.067 \pm 0.011 \quad \text{and} \quad \alpha_S(36.6\ \mathrm{GeV}) = 0.150 \pm 0.020 \tag{8}$$

at the luminosity weighted average centre-of-mass energy of 36.6 GeV where the errors are from the fit, and where $\eta^{\mathrm{ch}} = 0.6196 \pm 0.0043$ was obtained in both fits. The fitted value of η^{ch} agrees within errors with the expectation of the JETSET Monte Carlo generator in Eq. (5). A significant correlation of η^{ch} with α_S and $\sigma_L/\sigma_{\mathrm{tot}}$ of -77% is present. The correlation increases when smaller fit ranges are chosen. This signals a reduced ability of the fit to distinguish the longitudinal contribution to the cross-section from a simple change of the normalization. The result for the transverse cross-section can be derived from Eq. (8) with Eq. (4) and is therefore exactly anti-correlated to the longitudinal cross-section.

Besides the errors propagated from the measured $q \cdot \cos\theta$ distribution the fits were repeated for every systematic variation of the measurement. Deviations with respect to the standard fit results were taken as systematic uncertainties. Several other fit ranges, $|\cos\theta| < 0.52 \ldots 0.80$ were considered. The largest up- and downward excursion from the standard result was assigned as the uncertainty due to the choice of the fit range. Due to the correlation between the two fit parameters, the value of η^{ch} was kept fixed at 0.6196 for the variation of the fit ranges. Otherwise the reduced discrimination power between η^{ch} and α_S ($\sigma_L/\sigma_{\mathrm{tot}}$) for small fit ranges biases the estimation of this uncertainty. The 1.6% difference in the correction of the longitudinal and transverse cross-sections for the contribution of neutral particles was examined by introducing η_L^{ch} and η_T^{ch} obeying the relation $\eta_T^{\mathrm{ch}} = 1.016\eta_L^{\mathrm{ch}}$ in the fit formula Eq. (6). This yielded a negligible contribution to the overall systematic uncertainties. For the α_S determination an additional uncertainty arises from the choice of the renormalization scale, which was varied

[2] Using the statistical errors of the data only gave $\chi^2/\mathrm{d.o.f.} \approx 0.89$

	$\sigma_L/\sigma_{\text{tot}}$	$\sigma_T/\sigma_{\text{tot}}$	$\alpha_S(36.6\text{ GeV})$
fit result	0.067	0.933	0.150
data statistics	± 0.009	∓ 0.009	± 0.016
MC statistics	± 0.007	∓ 0.007	± 0.012
total stat. error	± 0.011	∓ 0.011	± 0.020
$p > 0.2$ GeV	< 0.001	< 0.001	< 0.001
$n_{\text{ch}}^{\text{vertex}} > 7$	< 0.001	< 0.001	$+0.001$
$n_{\text{ch}} > 7$	$+0.006$	-0.006	$+0.011$
$E_{\text{vis}} > (0.95 \ldots 1.05) \cdot \sqrt{s}/2$	± 0.001	∓ 0.001	± 0.001
$p_{\text{bal}} < (0.3 \ldots \infty)$	± 0.002	∓ 0.002	± 0.004
$\|z_{\text{VTX}} - \langle z_{\text{VTX}} \rangle\| < (29 \ldots 39)$ mm	$+0.002$	-0.002	$+0.004$
$\|\cos\theta_T\| < (0.7 \ldots 0.9)$	$^{+0.001}_{-0.006}$	$^{-0.001}_{+0.006}$	$^{+0.003}_{-0.010}$
$p_{\text{miss}} < (0.25 \ldots \infty) \cdot \sqrt{s}$	± 0.001	∓ 0.001	± 0.002
$d_0 < (3 \ldots 19)$ mm	-0.001	$+0.001$	-0.003
$\eta_T^{\text{ch}} = 1.016 \cdot \eta_L^{\text{ch}}$	< 0.001	< 0.001	< 0.001
reweighting of fragmentation fct.	$+0.002$	-0.002	$+0.005$
fit range $\|\cos\theta\| < 0.52 \ldots 0.8$	± 0.001	± 0.001	± 0.002
total syst. error	± 0.007	∓ 0.007	± 0.013
$x_\mu = 0.5 \ldots 2$	—	—	± 0.008
total error	± 0.013	∓ 0.013	± 0.025

Table 4: Error contributions for the determinations of $\sigma_L/\sigma_{\text{tot}}$, $\sigma_T/\sigma_{\text{tot}}$, which are exactly anti-correlated, and of $\alpha_S(36.6\text{ GeV})$.

from $\mu = \sqrt{s}$ by a factor $x_\mu \equiv \mu/\sqrt{s} = 0.5$ or 2. The individual positive and negative systematic error contributions were added in quadrature and symmetrized for the final result.

The results with all alloted errors are

$$\begin{aligned} \frac{\sigma_L}{\sigma_{\text{tot}}} &= 0.067 \pm 0.011(\text{stat.}) \pm 0.007(\text{syst.}) \\ \alpha_S(36.6\text{ GeV}) &= 0.150 \pm 0.020(\text{stat.}) \pm 0.013(\text{syst.}) \pm 0.008(\text{scale}) \quad , \end{aligned} \tag{9}$$

where the third error on α_S is due to the variation of the renormalization scale. Tab. 4 shows the individual error contributions to the results which are dominated by the statistical error. In this table, the contributions of the statistical uncertainties due to data and Monte Carlo simulation are given separately to illustrate the possible gain from a larger sample of simulated events on the total errors.

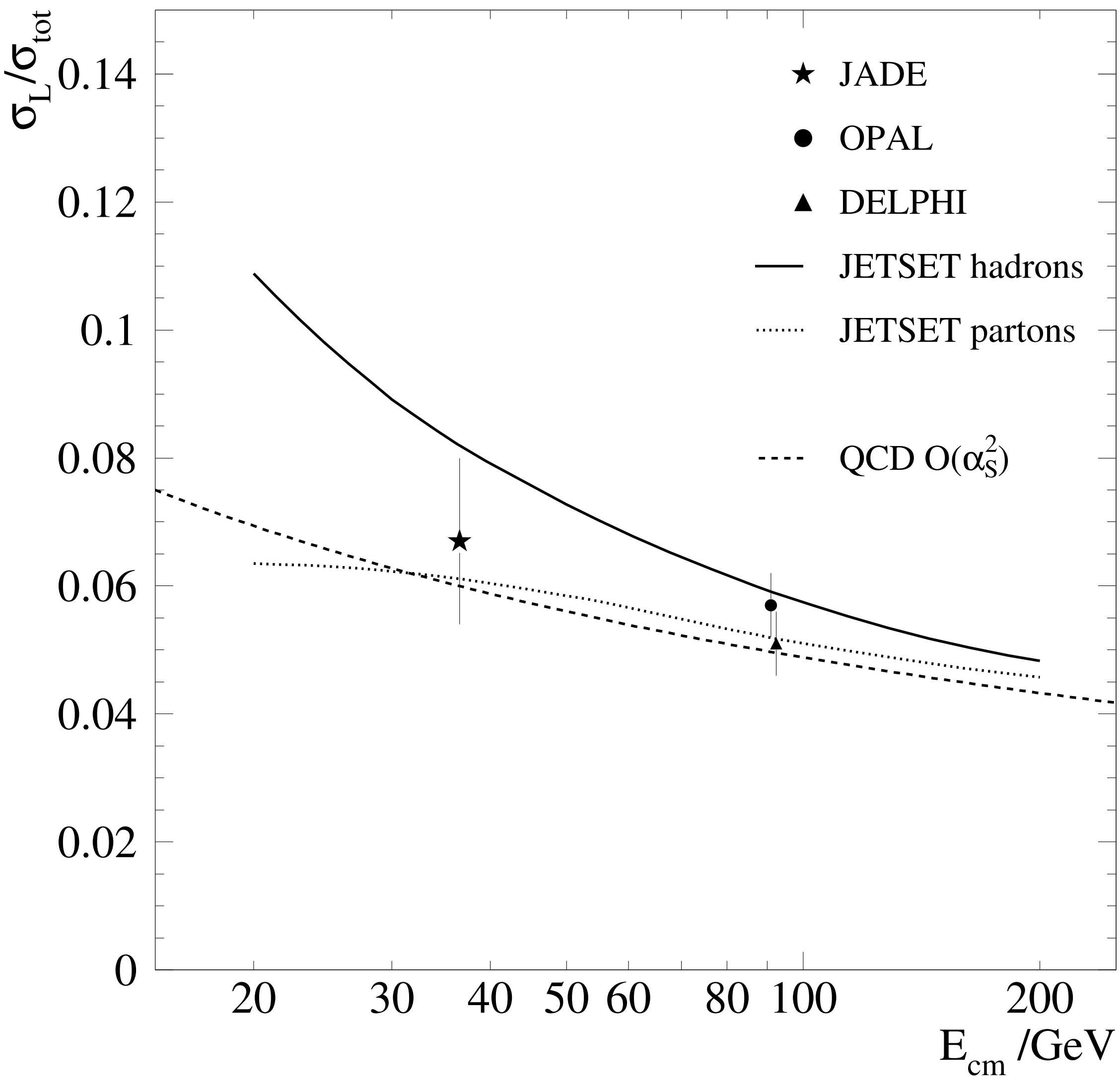

Figure 3: Longitudinal cross-section relative to the total cross-section is presented versus centre-of-mass energy. The results obtained at the Z peak [8,10] are also shown. The dotted and solid lines show, respectively, the JETSET[4] [14] expectation for partons and stable particles. The dashed line is the second order QCD prediction, Eq. (7), using $\alpha_S(m_Z) = 0.1184 \pm 0.0031$ [22].

5 Power correction

Fig. 3 shows our result and those obtained at the Z peak [8,10] for the ratio of the longitudinal and total cross-section versus the centre-of-mass energy. Neither the measurement of the SLAC/LBL magnetic detector [6] nor that of the TASSO collaboration [7] were considered for the study of power corrections. The results published by the SLAC/LBL collaboration, from which $\sigma_L/\sigma_{\rm tot} = 0.10 \pm 0.02(\text{stat.})$ at $\sqrt{s} = 7.4$ GeV can be derived, are solely quoted with statistical uncertainties. The TASSO collaboration used for their investigations a limited the x range of 0.02-0.3 only.

Even though the application of the sum rule, Eq. (2), should absorb all the details about the fragmentation functions a large difference exists between the JETSET expectations at parton and at hadron level. This indicates a substantial hadronization correction which is expected to

[4]Version 7.4 with tuned parameters from [17]

behave as a leading order $1/\sqrt{s}$ power correction [11].

For the study of the power correction to the longitudinal cross-section we used the parametrization of [18] where the power correction is given by

$$\frac{\sigma_L}{\sigma_{\rm tot}} = \left(\frac{\sigma_L}{\sigma_{\rm tot}}\right)_{\rm PT} + a_{\sigma_L} \cdot \frac{16\mathcal{M}}{3\pi^2}\frac{\mu_I}{\sqrt{s}} \cdot \left(\alpha_0(\mu_I) - \alpha_S(\mu) + \mathcal{O}(\alpha_S^2)\right) \quad . \tag{10}$$

Here $\mathcal{M} \approx 1.49$ is the Milan factor, μ_I, usually chosen to be 2 GeV, is the infrared matching scale of the non-perturbative term with the perturbative terms. The non-calculable parameter $\alpha_0(\mu_I)$ is to be determined from a fit to the data. The coefficient of the power correction for σ_L given in [19,20] is $a_{\sigma_L} = \pi/2$ when being adapted for the parametrization chosen in Eq. (10). Since the available $\sigma_L/\sigma_{\rm tot}$ data are not sufficiently precise for a detailed test of the power corrections, we solely quote for illustrative purposes the result $\alpha_S(m_{\rm Z})$ and $\alpha_0(2\ \text{GeV})$ from fitting the second order plus power correction prediction. This yielded:

$$\alpha_S(m_{\rm Z}) = 0.126 \pm 0.025 \quad \text{and} \quad \alpha_0(2\ \text{GeV}) = 0.3 \pm 0.3 \quad , \tag{11}$$

where the errors propagated from the total uncertainties of the $\sigma_L/\sigma_{\rm tot}$ data. With the large uncertainties and without further data no definite conclusion about the power correction for the longitudinal cross-section is possible. The size of the power correction expected at the Z peak was estimated to be $\delta^{\rm pow}(\sigma_L/\sigma_{\rm tot}) = 0.010 \pm 0.001$ [19] using the measured value of $\sigma_L/\sigma_{\rm tot}$ at $\sqrt{s} \approx m_{\rm Z}$ quoted in [8].

6 Summary

This paper presents the first measurement of the longitudinal and transverse cross-sections at PETRA energies of 35 through 44 GeV. Values of

$$\begin{aligned}\frac{\sigma_L}{\sigma_{\rm tot}} &= 0.067 \pm 0.011(\text{stat.}) \pm 0.007(\text{syst.}) \\ \frac{\sigma_T}{\sigma_{\rm tot}} &= 0.933 \mp 0.011(\text{stat.}) \mp 0.007(\text{syst.})\end{aligned} \tag{12}$$

were obtained for the longitudinal and transverse cross-sections relative to the total hadronic cross-section, where the errors are statistical and systematics. The two results are exactly anti-correlated since the relative transverse cross-section was obtained using the relation (4). The statistical errors are due to the data and the limited Monte Carlo simulation statistics which are about equal in size.

Using the second order QCD prediction for the relative longitudinal cross-section, a value of

$$\alpha_S(36.6\ \text{GeV}) = 0.150 \pm 0.020(\text{stat.}) \pm 0.013(\text{syst.}) \pm 0.008(\text{scal.}) \tag{13}$$

was determined for the strong coupling constant at the luminosity weighted average centre-of-mass energy of 36.6 GeV. Evolved to the Z peak using the 3-loop formula from [21] this result corresponds to $\alpha_S(m_{\rm Z}) = 0.127^{+0.017}_{-0.018}$ with total errors, which is in agreement with the current average $\alpha_S(m_{\rm Z}) = 0.1184 \pm 0.0031$ [22].

Power corrections to the longitudinal cross-section were considered. The available measurements at 36.6 GeV and 91.2 GeV are not sufficient yet for a definite conclusion.

Acknowledgements

M.B. thanks the members of the III. Physikalisches Institut of the RWTH Aachen for their generous hospitality and many helpful discussions.

References

[1] B. Naroska, Phys. Rep. **148** (1987) 67.

[2] P. Nason and B.R. Webber, Nucl. Phys., **B421** (1995) 473, Erratum: ibid, **B480** (1996) 755.

[3] G. Altarelli, Phys. Rep. **81** (1982) 1;
B. Mele and P. Nason, Nucl. Phys. **B361** (1991) 626.

[4] M. Böhm and W. Hollik (conv.) in: *Z Physics at LEP 1*, G. Altarelli, R. Kleiss, C. Verzegnassi (eds.), CERN 89-08, Vol. 1, (1989) 203.

[5] P.J. Rijken and W.L. van Neerven, Phys. Lett. **B386** (1996) 422.

[6] SLAC/LBL magnetic detector, R.F. Schwitters et al., Phys. Rev. Lett. **35** (1975) 1320.

[7] TASSO Collab., R. Brandelik et al., Phys. Lett. **B114** (1982) 65.

[8] OPAL Collab., R. Akers et al., Z. Phys. **C68** (1995) 203.

[9] ALEPH Collab., D. Buskulic et al., Phys. Lett. **B357** (1995) 487.

[10] DELPHI Collab., P. Abreu et al., Eur. Phys. J. **C6** (1999) 19.

[11] M. Beneke, V.M. Braun, and L. Magnea, Nucl. Phys. **B497** (1997) 297.

[12] JADE Coll., W. Bartel et al.: Phys. Lett. **88B** (1979) 171.
JADE Coll., W. Bartel et al.: Phys. Lett. **129B** (1983) 145.

[13] P.A. Movilla Fernández, O. Biebel, S. Bethke, S. Kluth, P. Pfeifenschneider and the JADE Collab.: Eur. Phys. J. **C1** (1998) 461.

[14] T. Sjöstrand: Comput. Phys. Commun. **39** (1986) 347,
T. Sjöstrand and M. Bengtsson: Comput. Phys. Commun. **43** (1987) 367.
We used version 6.3 of JETSET as used by the JADE collaboration with parameters from [16] to generate the events.

[15] JADE Collab., W. Bartel et al., Z. Phys. **C20** (1983) 187.

[16] JADE Collab., E. Elsen et al., Z. Phys. **C46** (1990) 349.

[17] OPAL Collab., G. Alexander et al., Z. Phys. **C69** (1995) 543.

[18] Yu.L. Dokshitzer, A. Lucenti, G. Marchesini, and G.P. Salam, Nucl. Phys. **B511** (1998) 396, hep-ph/9707532; J. High Energy Phys. **05** (1998) 003, hep-ph/9802381.

[19] Yu.L. Dokshitzer and B.R. Webber, Phys. Lett. **B352** (1995) 451, hep-ph/9504219.

[20] M. Dasgupta, L. Magnea, and G.E. Smye, J. High Energy Phys. **11** (1999) 025, hep-ph/9911316.

[21] Particle Data Group, D.E. Groom et al.: Eur. Phys. J. **C15** (2000) 1.

[22] S. Bethke: J. Phys. **G26** (2000) R27, hep-ex/0004021.